Catalysis Communications 154 (2021) 106310

Contents lists available at ScienceDirect

Catalysis Communications

journal homepage: www.elsevier.com/locate/catcom

Short communication

Synthesis of a high surface area and highly dispersed Cu-O-Si complex oxide used for the low-temperature hydrogenation of dimethyl oxalate to ethylene glycol

Yu Zhao [a,*,1], Xian Kan [a,1], Hongfei Yun [a], Dongliang Wang [a], Ning Li [a], Guixian Li [a,*], Jianyi Shen [b]

[a] School of Petrochemical Engineering, Lanzhou University of Technology, Lanzhou 730050, Gansu, China
[b] School of Chemistry and Chemical Engineering, Nanjing University, Nanjing 210093, Jiangsu, China

ARTICLE INFO

Keywords:
Cu-O-Si complex oxide
Atomic dispersion
Hydrogenation
Ethylene glycol
Low-temperature reaction

ABSTRACT

A highly dispersed Cu-O-Si composite oxide framework catalyst with high surface area (619 m^2/g) and very small particle size (~3 nm) has been synthesized using an improved precipitation method, which showed high catalytic activity toward the hydrogenation of dimethyl oxalate (DMO) (99.9% conversion of DMO and 96.7% selectivity for ethylene glycol) even at low temperature (175 °C). In addition, its chemical stability was significantly enhanced due to the formation of a Cu-O-Si composite structure and the low reaction temperature, and the catalyst did not show any significant inactivation during the stability test over 140 h.

1. Introduction

Ethylene glycol (EG) is an important chemical product that has versatile applications during the manufacture of polyester, lubricant and anti-freeze [1]. At present, the industrial production of EG is conducted via the hydration of ethylene oxide produced from petroleum-derived ethylene. With the depletion of petroleum resources and increasing demand for EG, the search for a new EG production method is increasingly imperative. Recently, the production of EG from coal has attracted more and more attention, in which the hydrogenation of dimethyl oxalate (DMO) to EG is the crucial step [2,3]. A considerable number of studies on catalysts have shown that the Cu/SiO_2 catalyst is the most promising candidate from the perspective of its environmental friendliness and high selectivity toward EG [4]. However, the poor stability of copper is an important factor affecting the wide use of Cu/SiO_2 catalysts [5]. As the Hüttig and Tamman temperatures of copper are relatively low, it easily moves under the reaction conditions and small granules may undergo aggregation to form large particles, resulting in a decrease in the catalytic activity [6]. Numerous methods have been developed to enhance the stability of copper-based catalysts [7–13]. Among them, the most common method is to dope a second component into the catalyst to stabilize the copper species and extend the lifespan of the catalyst by forming a metal solid solution or strengthen the interactions formed between the second metal species and Cu [14–16]. In addition, the synergistic effect of the second metal can also improve the catalytic activity and affect the product distribution. However, the incorporation of a second component makes the catalytic system complicated and increases the difficulty in understanding the catalytic reaction. Moreover, the technical control points in the catalyst preparation process are more complicated. Therefore, it is more advantageous to synthesize single metal Cu/SiO_2 catalysts with high stability. A possible method to improve the chemical stability of single metal Cu/SiO_2 catalysts is to embed the copper species into the framework of the silica support to form an atomically dispersed Cu-O-Si composite oxide framework. The strong interactions formed between copper, silicon and oxygen can limit the movement of copper, thus effectively improving the chemical stability of the copper species.

Herein, a series of highly dispersed Cu-O-Si composite oxide framework materials with high surface areas were successfully synthesized using a simple improved precipitation method. Based on the high catalytic activity as expected, a reduced reaction temperature (even at 175 °C) would be used for the hydrogenation of DMO. Thus, the chemical stability of the Cu-O-Si catalyst would be significantly enhanced due to the formation of the Cu-O-Si skeleton structure and the

---

* Corresponding authors at: School of Petrochemical Engineering, Lanzhou University of Technology, Lanzhou 730050, Gansu, China.
E-mail addresses: yzhao@lut.edu.cn (Y. Zhao), lgxwyf@163.com (G. Li).

[1] These authors contributed equally to this work.

https://doi.org/10.1016/j.catcom.2021.106310
Received 30 January 2021; Received in revised form 9 March 2021; Accepted 24 March 2021

Table 1
Physicochemical properties of the calcined catalyst samples.

Samples	Cu loading $(wt\%)$[a]	Cu dispersion (%)[b]	S_{BET} $(m^2 \cdot g^{-1})$[c]	d_p (nm)[c]	V_p $(cm^3 \cdot g^{-1})$[cy]
$CuSi_1$	8.75	/	354.7	13.0	1.49
$CuSi_2$	16.73	/	385.0	14.7	1.83
$CuSi_3$	24.09	40.95	619.5	10.3	2.37
$CuSi_4$	29.18	/	564.1	9.2	1.96
IM-CuSi	23.92	9.72	272.9	3.8	0.32

[a] Cu loading determined by ICP-OES.
[b] Cu dispersion determined by N_2O titration.
[c] Obtained by N_2 adsorption-desorption.

low reaction temperature. To the best of our knowledge, the strategy of enhancing the catalytic stability of the Cu/SiO_2 catalyst via reducing the reaction temperature has been rarely reported [17].

2. Experimental

2.1. Catalyst preparation

Cu-O-Si composite oxides with a preset copper-silicon atomic ratio varying from 0.1 to 0.4 were prepared using a precipitation method. Typically, 400 mL of deionized water was added to a three-necked flask and heated to 80 °C in an oil bath. An appropriate amount of $Cu(NO_3)_2{\cdot}3H_2O$ was dissolved in 100 mL of 2 mol/L nitric acid solution and 28.42 g $NaSiO_3{\cdot}9H_2O$ was dissolved in 150 mL of deionized water. The two solutions were added dropwise at the same time to the three-necked flask with stirring. The stirring was stopped after 1 h and the mixture was maintained at 80 °C for 12 h for crystal maturation. The precipitate was filtered and washed. It was then added to a beaker containing 200 mL of n-butanol and the mixture was heated to 110 °C under stirring to evaporate the solvent. After the evaporation process was completed, the precursor was dried at 110 °C overnight and then calcined at 450 °C in air for 4 h. Finally, the resulting solid was crushed and sieved to 40–60 mesh. The catalysts were denoted as $CuSi_1$, $CuSi_2$, $CuSi_3$ and $CuSi_4$, where one to four indicated that the copper-silicon atomic ratio of the samples was 0.1 to 0.4, respectively.

To compare the differences in the preparation method used, a contrast sample was prepared via an impregnation method and the sample obtained was labeled as IM-CuSi.

2.2. Characterization

The obtained samples were characterized using N_2 adsorption-desorption, XRD, TEM, H_2-TPR, XPS and XAES, N_2O chemisorptions, ICP-OES, etc. The detailed characterization process can be found in the supplementary information.

2.3. Catalytic activity

The hydrogenation of DMO was performed in a continuous-flow fixed-bed reactor and the condensed products were analyzed on an Agilent 3500GC instrument equipped with a flame-ionization detector, which can be seen in detail in the supplementary information.

3. Results and discussion

3.1. N_2 adsorption-desorption

The results of N_2 adsorption-desorption measurements for all the calcined samples are shown in Table 1, Figs. S1 and S2. The adsorption isotherms of the $CuSi_x$ samples exhibited typical type IV isotherms with H1-type hysteresis loops when the copper loading was low and a type-H3 hysteresis loop upon increasing the copper content [18]. $CuSi_3$ exhibited the largest specific surface area and pore volume among all the samples studied, which were 619 m^2/g and 2.37 cm^3/g, respectively, even if the Cu content was 24 wt% (see ICP results in Table 1). To the best of our knowledge, this is the largest specific surface area reported for single Cu-Si-O catalysts prepared using ammonia evaporation, precipitation-deposition, sol-gel, ion-exchange and impregnation methods. In contrast to $CuSi_3$, the specific surface area of the IM-CuSi sample with the same Cu content was only 273 m^2/g. The contrast between $CuSi_3$ and IM-CuSi clearly showed the superiority of our synthesis method. A large specific surface area and pore volume are pivotal bases for the good dispersion of Cu species on the catalyst [6]. Thus, $CuSi_3$ with the maximum specific surface area among all the $CuSi_x$ samples was selected as the catalyst for catalytic activity test described below.

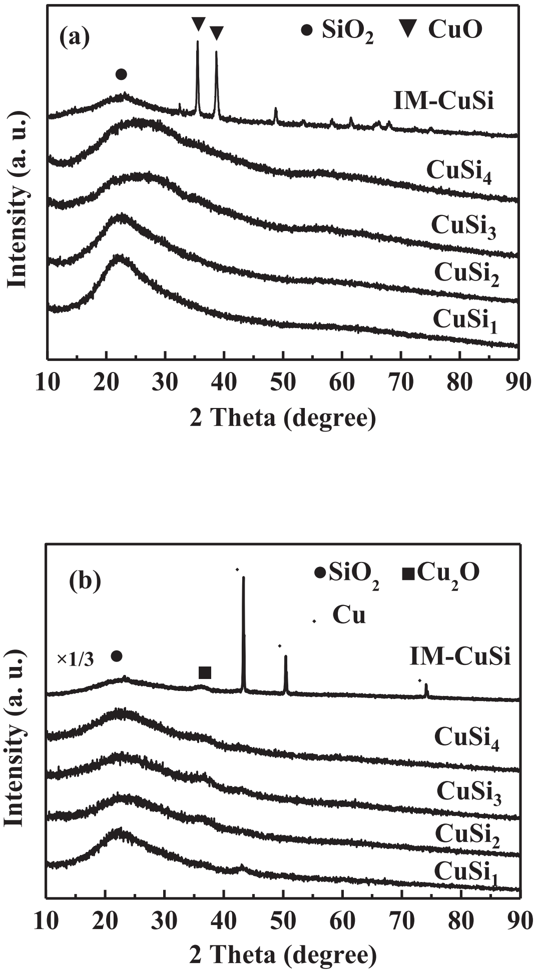

Fig. 1. XRD patterns obtained for the $CuSi_x$ and IM-CuSi samples (a) calcinated at 450 °C and (b) reduced at 350 °C.

3.2. XRD analysis

The XRD patterns obtained for the calcined and reduced $CuSi_x$ and IM-CuSi samples are shown in Fig. 1(a) and (b). For the calcined $CuSi_x$ samples, with the exception of the distinct diffraction peak observed at $2\theta = 22°$, which was ascribed to amorphous SiO_2, no diffraction peaks related to the copper species were detected, indicating that the copper species were well dispersed in the support. The high specific surface area of the catalysts should be responsible for the good dispersion of the copper species at a high copper content. An increase in the copper content usually deteriorates the dispersion of the copper species on the support, but the catalysts we synthesized maintain the good dispersion of the copper species even when the copper content was close to 30%.

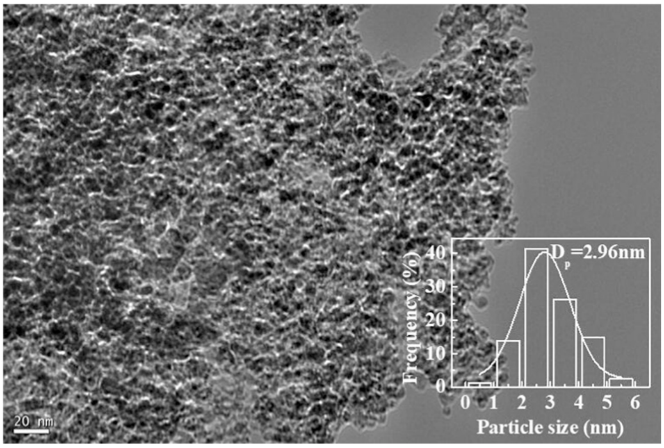

Fig. 2. The TEM image of the reduced $CuSi_3$ catalyst.

Those data indicated that the measures we took in the catalyst synthesis were effective toward improving the dispersion of the copper species. However, the XRD pattern of the calcined IM-CuSi sample showed two sharp peaks at $2\theta = 35.5°$ and $38.7°$, accompanied by satellite peaks at $48.8°$ and $61.5°$, which clearly indicated that there was a large amount of blocky CuO in the IM-CuSi sample [19].

The XRD patterns of the reduced samples are shown in Fig. 1(b). The diffraction patterns of the reduced $CuSi_x$ samples exhibited a very weak peak at 37.5°, which could be attributed to the Cu_2O species [19]. The peaks were weak and diffuse, indicating that the particle size of Cu_2O was small and the crystallinity was poor. During the reduction process, the forming Cu metallic species leave the silica framework, so sintering should always occur. However, due to the stable Cu-O-Si structure and enhanced strong metal-support interactions (SMSI) formed during the calcination treatment, the copper particle size in the $CuSi_x$ samples after the reduction step was still small. However, the XRD pattern of the reduced IM-CuSi sample showed sharp diffraction peaks at 43.3, 50.4 and 74.1°, which belonged to the Cu^0 species. The XRD pattern also showed weak diffraction at 37.5° corresponding to the Cu_2O species, indicating that the reduced IM-CuSi samples were mainly composed of large metallic Cu particles and a small amount of Cu_2O species.

3.3. Transmission electron microscopy (TEM)

The morphologies of the reduced $CuSi_3$ and IM-CuSi samples were investigated using TEM. In the case of the reduced $CuSi_3$ sample (Fig. 2), a large number of copper species were uniformly dispersed on the support and the particle size distribution showed that the average diameter of copper species on the sample was only 2.96 nm, which is consistent with the XRD pattern. However, the average diameter of copper species on the IM-CuSi catalyst was ~18 nm (Fig. S3). Apparently, the dispersion of copper species on the support for the IM-CuSi catalyst was poor, which may be a result from the weak interaction formed between the impregnated copper species and the support, and the severe agglomeration of the copper species during the calcination and reduction steps.

3.4. N_2O titration

The well dispersed Cu catalyst can produce high surface Cu^0 and Cu^+ concentrations combined with a high $Cu^+/(Cu^0 + Cu^+)$ ratio to achieve high catalytic activity [10]. Thus, the dispersion of surface copper in the $CuSi_3$ and IM-CuSi sample were compared using N_2O titration studies [20] and the results are listed in Table 1. The $CuSi_3$ sample possessed a high dispersion of copper (40.95%), which was much higher than that in the IM-CuSi sample (9.72%). The N_2 adsorption-desorption, XRD and TEM analyses showed that the $CuSi_3$ sample exhibited a significantly higher surface area and much smaller Cu particle size than the IM-CuSi sample. Thus, the high copper dispersion of the $CuSi_3$ sample was easy to understand.

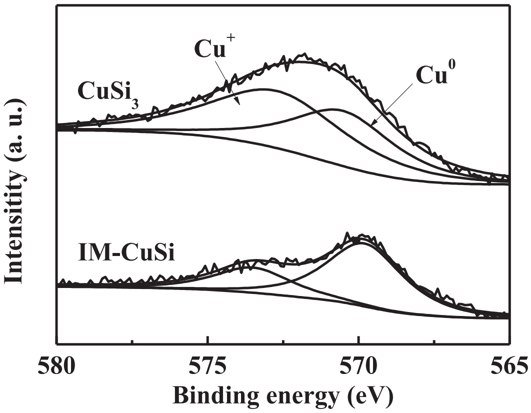

Fig. 3. Cu LMM Auger spectra obtained for the reduced $CuSi_3$ and IM-CuSi catalysts.

3.5. H_2-TPR analysis

H_2-TPR was performed to evaluate the reducibility of the calcined catalysts. Fig. S4 showed that the reduction peaks in $CuSi_x$ were all located in the low temperature region (200–300 °C), indicating that the copper species in these samples were made up of small particles that were easy to reduce. The H_2 consumption increased with an increase in the Cu contents from $CuSi_1$ to $CuSi_4$. The reduction behavior of the IM-CuSi sample was quite different from that of the $CuSi_x$ samples. The TPR curve of the IM-CuSi sample showed a reduction peak at 219 °C, corresponding to the reduction of copper species with small particle size in the IM-CuSi sample [21]. The reduction temperature was much lower than that of $CuSi_3$, indicating that the interactions formed between the copper species and the support were weak and these copper species were prone to be reduced. There were two additional broad hydrogen consumption peaks in the high temperature regions of 260–330 °C and 375–425 °C, which could be attributed to the large particles of CuO with poor dispersion in the IM-CuSi sample. In addition, the H_2 consumption observed for the IM-CuSi sample was larger than that for the $CuSi_3$ sample with the same Cu content, indicating that some Cu^+ species may already exist in the calcined $CuSi_3$ sample due to the strong interactions among the Cu-O-Si composite structure.

3.6. XPS analysis

The surface chemical states of the reduced $CuSi_3$ and IM-CuSi samples were determined using XPS. As seen in Fig. S5, Cu^{2+} was completely reduced to its low valence state after the reduction process [22]. Further research on the Cu Auger LMM spectra shown in Fig. 3 indicates that all the spectra present a series of asymmetrical and broad peaks, indicating the coexistence of Cu^+ and Cu^0 on the surface of the catalysts. Deconvolution of the Cu LMM peaks was carried out and the peak located at 569.8 eV corresponded to the Cu^0 species, while the peak with a higher BE value was the peak corresponding to the Cu^+ species [23]. The deconvolution results showed that the Cu^+ content on the surface of the reduced $CuSi_3$ (58.3%) and IM-CuSi samples (28.6%) differed greatly. It was the special Cu-O-Si structure in the $CuSi_3$ sample, which strongly interacted with the support, retarding the further reduction of Cu^+ into Cu^0.

3.7. Catalytic performance during the hydrogenation of DMO

The hydrogenation of DMO was performed to compare the catalytic performance of the catalysts and the reaction can be seen in Scheme S1

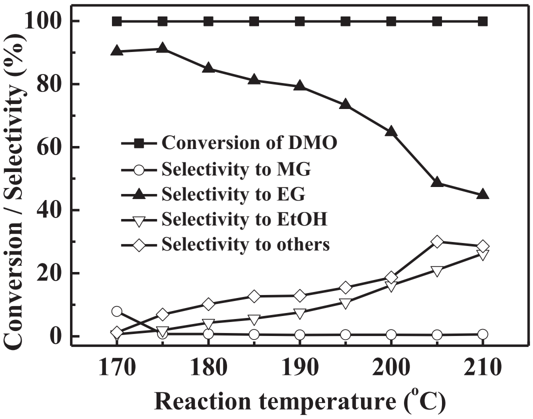

Fig. 4. Effect of reaction temperature on the catalytic performance over $CuSi_3$ catalyst. Reaction conditions: P = 2.5 MPa, LHSV = 0.5 h^{-1} and H_2/DMO = 120.

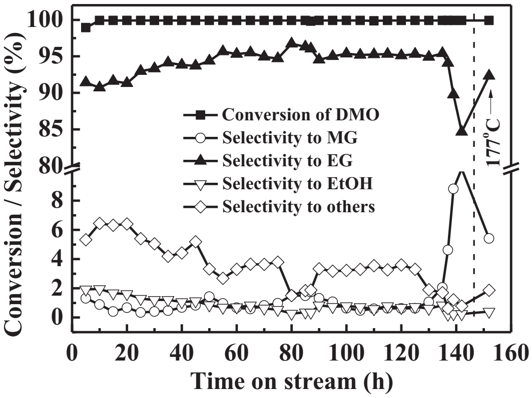

Fig. 5. Stability test for the $CuSi_3$ catalyst. Reaction conditions: P = 2.5 MPa, LHSV = 0.5 h^{-1}, T = 175 °C and H_2/DMO = 120.

in the supplementary information. Firstly, the traditional reaction temperature (200 °C) was used and the results are shown in Fig. S6 and S7, which indicate that $CuSi_3$ possessed much higher catalytic activity than that for the IM-CuSi catalyst. Based on these results, the hydrogenation of DMO at low temperature with an LHSV of 0.5 h^{-1} over the $CuSi_3$ catalyst was subsequently carried out. It is amazing that the conversion of DMO and the selectivity toward EG can reach 99.9% and 91.1%, respectively, even at a low temperature (175 °C) (Fig. 4). For comparison, the hydrogenation of DMO hardly occurs over the IM-CuSi catalyst under the same reaction conditions. To the best of our knowledge, the hydrogenation of DMO to EG at 175 °C has been rarely reported over the Cu/SiO_2 catalyst, let alone such high conversion of DMO and selectivity toward EG. Considering that the poor stability of Cu/SiO_2 catalysts is probably due to the low Hüttig and Tamman temperatures of copper, the low-temperature reaction can obviously improve the catalytic stability of the Cu/SiO_2 catalyst. Thus, the stability test of $CuSi_3$ was further studied at 175 °C and the results shown in Fig. 5. It can be seen that after 135 h of reaction, the conversion of DMO remained at 99.9% and the selectivity toward EG remained at ~95.0% (the highest one reached 96.7%), but in the range of 135–142 h, the selectivity toward EG slightly decreased to 84.6%. It is worth noting that the selectivity toward EG could be recovered to 92.3% with a slight temperature compensation of only 2 °C, that is, when performing the reaction at 177 °C. Thus, the enhancement of the catalytic stability for the monometallic Cu/SiO_2 catalyst with high catalytic activity via reducing the reaction temperature is a promising strategy for academic and industrial considerations.

4. Conclusions

Cu-O-Si catalyst materials with large specific surface areas and highly dispersed metal species have been prepared using an improved precipitation method. The $CuSi_3$ catalyst prepared with a Cu content of 24 wt% possessed a much higher specific surface (619 m^2/g) and very small particle size (~3 nm), which exhibited high catalytic activity toward the hydrogenation of DMO with a DMO conversion of 99.9% and EG selectivity of 96.7% even at 175 °C. In addition, the formation of the Cu-O-Si composite structure and the low-temperature reaction significantly enhanced its chemical stability, and the catalyst did not show any significant inactivation during the stability test over 140 h. These results provide a new strategy to prepare highly stable single metal Cu/SiO_2 catalysts with high catalytic activity, which was much simpler than the conventional method of doping a second metal species to improve the stability of copper catalysts.

Declaration of Competing Interest

The authors declare that there is no conflict of interest.

Acknowledgements

Financial supports from Key research and development program in Gansu Province (18YF1GA062) and NSFC (21763016) are acknowledged.

Appendix A. Supplementary data

Supplementary data to this article can be found online at https://doi.org/10.1016/j.catcom.2021.106310.

References

[1] H.R. Yue, Y.J. Zhao, X.B. Ma, J.L. Gong, Ethylene glycol: properties, synthesis, and applications, Chem. Soc. Rev. 41 (2012) 4218–4244.

[2] Y. Huang, H. Ariga, X.L. Zheng, X.P. Duan, S. Takakusagi, K. Asakura, Y.Z. Yuan, Silver-modulated SiO_2-supported copper catalysts for selective hydrogenation of dimethyl oxalate to ethylene glycol, J. Catal. 307 (2013) 74–83.

[3] R.P. Ye, L. Lin, L.C. Wang, D. Ding, Z.F. Zhou, P.B. Pan, Z.H. Xu, J. Liu, H. Adidharma, M. Radosz, M.H. Fan, Y.G. Yao, Perspectives on the active sites and catalyst design for the hydrogenation of dimethyl oxalate, ACS Catal. 10 (2020) 4465–4490.

[4] Y.N. Wang, X.P. Duan, J.W. Zheng, H.Q. Lin, Y.Z. Yuan, H. Ariga, S. Takakusagi, K. Asakura, Remarkable enhancement of Cu catalyst activity in hydrogenation of dimethyl oxalate to ethylene glycol using gold, Catal. Sci. Technol. 2 (2012) 1637–1639.

[5] H.R. Yue, Y.J. Zhao, S. Zhao, B. Wang, X.B. Ma, J.L. Gong, A copper-phyllosilicate core-sheath nanoreactor for carbon–oxygen hydrogenolysis reactions, Nat. Commun. 4 (2013) 2339.

[6] H.R. Yue, Y.J. Zhao, L. Zhao, J. Lv, S.P. Wang, J.L. Gong, X.B. Ma, Hydrogenation of dimethyl oxalate to ethylene glycol on a Cu/SiO_2/cordierite monolithic catalyst: enhanced internal mass transfer and stability, AIChE J. 58 (2012) 2798–2809.

[7] X.B. Yu, T.A. Vest, N. Gleason-Boure, S.G. Karakalos, G.L. Tate, M. Burkholder, J. R. Monnier, C.T. Williams, Enhanced hydrogenation of dimethyl oxalate to ethylene glycol over indium promoted Cu/SiO_2, J. Catal. 380 (2019) 289–296.

[8] R.P. Ye, L. Lin, J.X. Yang, M.L. Sun, F. Li, B. Li, Y.G. Yao, A new low-cost and effective method for enhancing the catalytic performance of Cu-SiO_2 catalysts for the synthesis of ethylene glycol via the vapor-phase hydrogenation of dimethyl oxalate by coating the catalysts with dextrin, J. Catal. 350 (2017) 122–132.

[9] Y.Y. Cui, B. Wang, C. Wen, X. Chen, W.L. Dai, Investigation of activated-carbon-supported copper catalysts with unique catalytic performance in the hydrogenation of dimethyl oxalate to methyl glycolate, ChemCatChem 8 (2016) 527–531.

[10] J. Ding, T. Popa, J.K. Tang, K.A.M. Gasem, M.H. Fan, Q. Zhong, Highly selective and stable Cu/SiO_2 catalysts prepared with a greenmethod for hydrogenation of diethyl oxalate into ethylene glycol, Appl. Catal. B 209 (2017) 530–542.

[11] A. Chirieac, B. Dragoi, A. Ungureanu, C. Ciotonea, I. Mazilu, S. Royer, A. S. Mamede, E. Rombi, I. Ferino, E. Dumitriu, Facile synthesis of highly dispersed and thermally stable copper-based nanoparticles supported on SBA-15 occluded with P123 surfactant for catalytic applications, J. Catal. 339 (2016) 270–283.

[12] C.C. Chen, L. Lin, R.P. Ye, M.L. Sun, J.X. Yang, F. Li, Y.G. Yao, Mannitol as a novel dopant for Cu/SiO_2: a low-cost, environmental and highly stable catalyst for dimethyl oxalate hydrogenation without hydrogen prereduction, J. Catal. 389 (2020) 421–431.

[13] M.L. Wang, D.W. Yao, A.T. Li, Y.W. Yang, J. Lv, S.Y. Huang, Y. Wang, X.B. Ma, Enhanced selectivity and stability of Cu/SiO_2 catalysts for dimethyl oxalate

hydrogenation to ethylene glycol by using silane coupling agents for surface modification, Ind. Eng. Chem. Res. 59 (2020) 9414–9422.

[14] C.C. Chen, L. Lin, R.P. Ye, L. Huang, L.B. Zhu, Y.Y. Huang, Y.Y. Qin, Y.G. Yao, Construction of Cu-Ce composite oxides by simultaneous ammonia evaporation method to enhance catalytic performance of Ce-Cu/SiO_2 catalysts for dimethyl oxalate hydrogenation, Fuel 290 (2021) 120083.

[15] X.P. Wang, M. Chen, X.K. Chen, R.H. Lin, H.J. Zhu, C.Q. Huang, W.S. Yang, Y. Tan, S.S. Wang, Z.N. Du, Y.J. Ding, Constructing copper-zinc interface for selective hydrogenation of dimethyl oxalate, J. Catal. 383 (2020) 254–263.

[16] Y.J. Zhao, H.H. Zhang, Y.X. Xu, S.N. Wang, Y. Xu, S.P. Wang, X.B. Ma, Interface tuning of Cu^+/Cu^0 by zirconia for dimethyl oxalate hydrogenation to ethylene glycol over Cu/SiO_2 catalyst, J. Energy Chem. 49 (2020) 248–256.

[17] G.Q. Cui, X.Y. Meng, X. Zhang, W.L. Wang, S.L. Xu, Y.C. Ye, K.J. Tang, W.M. Wang, J.H. Zhu, M. Wei, D.G. Evans, X. Duan, Low-temperature hydrogenation of dimethyl oxalate to ethylene glycol via ternary synergistic catalysis of Cu and acid−base sites, Appl. Catal. B 248 (2019) 394–404.

[18] C.H. Cheng, G.X. Li, D. Ji, Y. Zhao, J.Y. Shen, Regulating hierarchical structure and acidity of HZSM-5 for methanol to aromatics via protective desiliconization and external surface modification, Micropor. Mesopor. Mat. 312 (2021) 110784.

[19] Y.J. Zhao, S.M. Li, Y. Wang, B. Shan, J. Zhang, S.P. Wang, X.B. Ma, Efficient tuning of surface copper species of Cu/SiO_2 catalyst for hydrogenation of dimethyl oxalate to ethylene glycol, Chem. Eng. J. 313 (2017) 759–768.

[20] Z.L. Yuan, L.N. Wang, J.H. Wang, S.X. Xia, P. Chen, Z.Y. Hou, X.M. Zheng, Hydrogenolysis of glycerol over homogenously dispersed copper on solid base catalysts, Appl. Catal. B-Environ. 101 (2011) 431–440.

[21] L.Y. Chen, T. Horiuchi, T. Osaki, T. Mori, Catalytic selective reduction of NO with propylene over Cu-Al_2O_3 catalysts: influence of catalyst preparation method, Appl. Catal. B 23 (1999) 259–269.

[22] L.F. Chen, P.J. Guo, M.H. Qiao, S.R. Yan, H.X. Li, W. Shen, H.L. Xu, K.N. Fan, Cu/SiO_2 catalysts prepared by the ammonia-evaporation method: texture, structure, and catalytic performance in hydrogenation of dimethyl oxalate to ethylene glycol, J. Catal. 257 (2008) 172–180.

[23] A.Y. Yin, X.Y. Guo, W.L. Dai, K.N. Fan, The nature of active copper species in Cu-HMS catalyst for hydrogenation of dimethyl oxalate to ethylene glycol: new insights on the synergetic effect between Cu^0 and Cu^+, J. Phys. Chem. C 113 (2009) 11003–11013.